

# Design of Magnetic Integrated LLC Transformer

Liang Xu\*, Dong Qing Miao, Jing Qiu Zhang

Zhongtian Broadband Technology Co., Ltd., Nantong 226400, Jiangsu, China

\*Corresponding author: Liang Xu, 1260523490@qq.com

**Copyright:** © 2023 Author(s). This is an open-access article distributed under the terms of the Creative Commons Attribution License (CC BY 4.0), permitting distribution and reproduction in any medium, provided the original work is cited.

**Abstract:** The direct current/direct current (DC/DC) converter of the LLC (inductor-inductor-capacitor) converter is an important part of affecting the work efficiency, volume, and weight of the device. It not only has the functions of traditional transformers but is also able to solve the problems of traditional power transformers' high price, huge volume, prodigious no-load loss, and inflexible control. This paper studies the DC/DC converter mainly, according to the given indexes, the magnetic integrated LLC resonant transformer is designed in detail. The magnetic integrated transformer greatly reduces the converter volume, and the selection of devices is completed based on parameters design. In addition, according to design parameters, losses and the efficiency of the LLC resonant transformer are calculated. The results meet the efficiency requirements. A test platform of a full-bridge LLC resonant converter is built according to theoretical research. The correctness and effectiveness of theoretical research and design methods of the DC/DC converter are verified by analyzing the experimental waveforms.

**Keywords:** DC/DC; LLC resonant converter; Loss analysis; Magnetic integrated transformer

**Online publication:** June 28, 2023

## 1. Introduction

The power supply system of the communication equipment room is very complex. To meet the requirements of different voltage levels <sup>[1]</sup>, traditional power transformers are currently commonly used for voltage transformation and energy transfer. This type of transformer has a simple manufacturing process and high reliability, but it is costly, large in volume, with severe no-load loss, and inflexible control. Moreover, if there are phenomena such as voltage imbalance, harmonics, flicker, etc., it cannot maintain the normal operation of power equipment <sup>[2]</sup>. It is crucial to ensure electrical equipment provides reliable and stable electricity to users safely <sup>[3]</sup>, whereby the direct current/direct current (DC/DC) converter emerged. In addition to possessing the functions of traditional transformers, it also can solve the aforementioned problems. As a new type of transformer, the LLC transformer, which had 2 inductances (L) and a capacitor (C), has become a hot research topic for scholars both domestically and internationally in recent years <sup>[4-8]</sup>. LLC topology, as a dual-ended resonant topology, has been applied in many DC/DC power conversion schemes. This study will design a DC/DC based on the principle of an LLC full bridge DC/DC converter, utilizing the advantages of the LLC resonant converter itself to improve DC/DC efficiency.

## 2. Working principle of LLC resonant full bridge converter

### 2.1. Introduction to the circuit structure

The main circuit topology of the LLC resonant full bridge converter is shown in **Figure 1**. During the working process, the excitation inductance  $L_m$  may be clamped and not participate in the operation, which determines that the LLC resonant converter will have two different resonant frequencies. When  $L_m$  is

clamped, which is generated by the resonant inductance  $L_r$  and the resonant capacitor  $C_r$ . The expression is:

$$f_r = \frac{1}{2\pi\sqrt{L_r C_r}}$$

When the current flowing through  $L_r$  is equal to the current flowing through the resonant inductor  $L_m$ , the transformer has no energy transmission, the rectifier tube will be turned off, and  $L_m$  will not be clamped by the secondary voltage to participate in resonance. At this time, the resonance frequency is related to the excitation inductance  $L_m$ , resonant inductance  $L_r$ , and resonant capacitor  $C_r$ . The expression is:

$$f_m = \frac{1}{2\pi\sqrt{(L_m + L_r)C_r}}$$

For LLC resonant full bridge converters, they can operate in four operating modes. Assuming the operating frequency is  $f_s$ , its relationship with the two resonant frequencies above will determine the range in which the converter operates. The relationship includes four situations:  $f_s \leq f_m$ ,  $f_m < f_s < f_r$ ,  $f_s = f_r$ ,  $f_s > f_r$ .

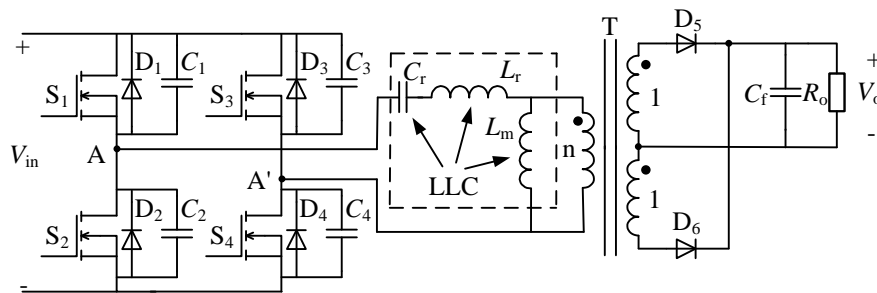


Figure 1. Schematic diagram of LLC full bridge converter

### 3. Design of LLC full bridge converter

In order to apply to the commonly used voltage levels in communication equipment rooms, the design of LLC resonant converters meets the following design indicators:

- (1) Input voltage range:  $V_{in\_min} \sim V_{in\_max} = 190 \sim 330$  V
- (2) Rated input voltage:  $V_{in\_nom} = 300$  V
- (3) Expected efficiency,  $\eta$ :  $\geq 95\%$
- (4) Output voltage:  $V_o = 48$  V
- (5) Ripple voltage:  $\Delta V = 240$  mV
- (6) Output current:  $I_o = 10$  A
- (7) Resonant frequency:  $f_r = 100$  kHz,  $k = 6$
- (8) Parasitic capacitance  $C_{oss}$  of metal-oxide-semiconductor field-effect transistor (MOSFET): 400 pF
- (9) Equivalent parasitic capacitance  $C_{stary}$  of transformer winding and PCB board: 100 pF
- (10) Dead time: 300 ns

#### 3.1. Design of resonant circuit parameters

To meet the input voltage working near  $f_r$  at  $V_{in\_nom}$ , the theoretical transformation ratio  $m$  of the transformer can be obtained by using the following equation with the gain  $M_{nom} = 1$  at this time, whereas  $V_F$  is the conduction voltage drop of the secondary diode, where 1 V is taken.

$$m = \frac{V_{in\_nom}}{(V_o + V_F)} = \frac{300}{(48+1)} = 6.12 \text{ V}$$

The minimum gain  $M_{min}$  and maximum gain  $M_{max}$  of the equivalent circuit are shown here:

$$M_{min} = m \frac{V_o + V_F}{V_{in\_max}} = 0.91$$

$$M_{max} = m \frac{V_o + V_F}{V_{in\_min}} = 1.58$$

The minimum operating frequency  $f_{min}$  and maximum operating frequency  $f_{max}$  of the equivalent circuit are as follows:

$$f_{min} = \frac{f_r}{\sqrt{1+k\left(1-\frac{1}{M_{max}^2}\right)}} = 46.64 \text{ kHz}$$

$$f_{max} = \frac{f_r}{\sqrt{1+k\left(1-\frac{1}{M_{min}^2}\right)}} = 156.83 \text{ kHz}$$

Based on the first harmonic approximation (FHA) analysis method, the equivalent load impedance of LLC circuits is as follows, where  $n$  is the theoretical transformation ratio of the transformer.

$$R_{ac} = \frac{8n^2V_o}{\pi^2I_o} = \frac{8 \times 6.12^2 \times 48}{\pi^2 \times 10} = 145.87 \ \Omega$$

According to the requirement of maximum gain, the maximum quality factors  $Q_{max1}$  and  $Q_{max2}$  of the resonant cavity can be obtained through the following equations, where  $k$  is the ratio of excitation inductance to resonant inductance,  $k = 6$ ;  $l_{max}$  is the maximum normalized frequency.

$$Q_{max1} = \frac{1}{kM_{max}} \sqrt{k + \frac{M_{max}^2}{M_{max}^2 - 1}} = 0.29$$

$$Q_{max2} = \frac{4t_d}{\pi R_{ac} C_{ZVS} \left( l_{max} - \frac{1}{l_{max}} + k l_{max} \right)} = 0.285$$

Hence, the maximum Q within the entire working range is  $Q_{ZVS} = 0.95 \times \min\{Q_{max1}, Q_{max2}\} = 0.27$ , where ZVS is defined as zero voltage switching. According to the resonance characteristics, the resonance parameters can be obtained as follows:

$$C_r = \frac{1}{2\pi f_r Q n^2 R_{ac}} = 40.03 \text{ nF}$$

$$L_r = \frac{QR_{ac}}{2\pi f_r} = 62.72 \mu\text{H}$$

$$L_m = kL_r = 376.32 \mu\text{H}$$

According to the conditions for achieving ZVS with the original side switch, the excitation current can be calculated as:

$$I_m = \frac{V_{in\_max}}{4f_{max}(L_m + L_r)} = 1.20 \text{ A}$$

The charging current of parasitic capacitors is:

$$I_p = C_{ZVS} \frac{V_{in\_max}}{t_d} = 0.98 \text{ A}$$

Since  $I_m > I_p$  meets the conditions for achieving ZVS in the primary side switch, the design is considered reasonable.

### 3.2. Design of magnetic integrated transformer

Integrated LLC resonant converter integrates the resonant inductance and excitation inductance into the transformer for utilizing the leakage inductance and excitation inductance of the transformer fully. Using the magnetic integration approach to integrate LLC resonant converters precisely utilizes the parasitic parameters of the transformer, where using the leakage inductance of the transformer as  $L_r$  and the excitation inductance of the transformer as  $L_m$ . This converts unfavorable factors into favorable conditions without adding two additional inductors, greatly reducing the volume of the converter. Area product (AP) method [11] is used to determine the type of transformer magnetic core, which is shown in the following equation:

$$AP = A_e A_w = \left[ \frac{P_T \times 10^4}{K_o K_f K_j f_s B_w} \right]^{1.14}$$

In the above formula,  $A_e$  is the effective cross-sectional area of the magnetic core;  $A_w$  is the window area of the coil;  $P_T$  is the apparent power of the transformer, which varies with the circuit. In this paper, the secondary side of the transformer adopts a central tap structure, so  $P_T = P_o(1/\eta + \sqrt{2})$ , unit W;  $K_o$  is the window utilization coefficient, taken as  $K_o = 0.3$ ;  $K_f$  is the waveform coefficient, which is 4 for the square wave.  $K_j$  is the current density, where  $K_j = 400/\text{cm}^2$ ;  $B_w$  is the working magnetic flux density,  $B_w = 0.15 \text{ T}$ . Bringing the data into the above equation yields can get:

$$AP = \left[ \frac{480 \times \left( \frac{1}{0.95} + \sqrt{2} \right) \times 10^4}{0.3 \times 4 \times 40 \times 100,000 \times 0.15} \right]^{1.14} = 1.76 \text{ cm}^4$$

ETD39 from TDK Electronics is used as a magnetic core, hence  $AP = 3.2125 \text{ cm}^4$ ,  $A_e = 1.25 \text{ cm}^2$ ,  $A_w = 2.57 \text{ cm}^2$ , and  $\Delta B = 0.3 \text{ T}$ . By adding the secondary leakage inductance to the primary inductance, the actual transformation ratio  $n$  of the transformer can be obtained using the following equation:

$$n = m \sqrt{\frac{k+1}{k}} = 6.61$$

According to the law of electromagnetic induction, the number of secondary turns can be obtained as:

$$N_s = \frac{V_o + V_F}{2f_{\min} \Delta B A_e} = 14.01$$

Hence, the roundup secondary turn count is 14 turns. According to the transformer ratio, the number of primary turns can be calculated as  $N_p = nN_s = 92.59$ , giving the roundup primary turn count of 92 turns.

Considering the influence of the skin effect, 64 strands of enameled wire ( $\Phi = 0.11$  mm) are wound in parallel on the primary side, whereas the secondary side is made of 63 strands of enameled wire ( $\Phi = 0.2$  mm). It not only meets the current stress but also reduces the loss caused by the skin effect.

In order to maximize the leakage inductance of the transformer and meet the requirements of the resonant inductance  $L_r$ , it is necessary to reduce the coupling degree of the primary and secondary sides. A combination of slot skeleton and retaining wall can be used to meet the requirements.

### 3.3. Selection of MOSFET and rectifier diodes

In a full bridge converter, the maximum voltage borne by MOSFET is the maximum input DC voltage, which is the peak value of MOSFET voltage, hence  $V_{ds\_max} = V_{in\_max} = 326$  V. The peak value of MOSFET current is  $I_{ds\_max} = \sqrt{2} I_{p\_RMS} = 3.17$  A. According to 1.5 times the withstand voltage value and 2 times the current value, the CoolMOS-IPW65R041CFD designed by Infineon was selected, with a withstand voltage of 650 V and a maximum conduction resistance of only 41 m $\Omega$ .

Rectifier diodes need to achieve zero current switching (ZCS) in high-frequency environments, which is difficult for ordinary diodes. Therefore, it is necessary to choose a fast recovery diode, which can withstand a maximum reverse voltage of 2 times the output voltage, where  $V_D = 2V_o = 96$  V. Maximum value of current flowing through the diode is  $I_{D\_max} = \sqrt{2} I_{s\_RMS} = 11.1$  A.

Considering a certain margin, MUR2020 was ultimately selected as the output rectifier diode, with a maximum withstand voltage of 200 V and a maximum average current that can withstand 20 A,  $V_F = 1.0$  V.

### 3.4. Output capacitor design

From the topology and working principle of the full bridge LLC resonant converter, it can be seen that its output only requires capacitor filtering, and the capacitor value is closely related to the output voltage ripple. When the expected ripple  $\Delta V \leq 240$  mV, the output capacitance is determined as follows, where  $\Delta V$  is the expected ripple value, and  $T_{s\_max}$  is the period corresponding to the maximum switching cycle.

$$C_o = \frac{I_o T_{s\_max}}{\Delta V} = 890 \mu\text{F}$$

In order to minimize the loss on the capacitor as much as possible, a capacitor with low ESR is selected. Nippon Chemi-Con 1000  $\mu\text{F}$  electrolytic capacitor with low ESR is selected, where the withstand voltage value is 63 V and ESR is 19 m $\Omega$ . The actual ripple value is  $\Delta V_2 = I_{c\_rms} R_{esr} = 0.092$  V, where  $I_{c\_rms}$  is the effective value of the current flowing through the capacitor, which can be obtained by the following equation:

$$I_{c\_rms} = \sqrt{\frac{\pi^2 - 8}{8}} I_o$$

Therefore, the ripple of the output voltage meets the expected requirements.

### 3.5. Loss and efficiency calculation

#### 3.5.1. MOSFET loss calculation

Due to the use of soft switching technology in this design, the switching loss of the circuit system is zero, and the loss of the MOSFET is only its conduction loss, which is  $P_{cond,MOSFET} = I_{d,rms}^2 R_{on} D = 0.1$  W. The  $R_{on}$  is the maximum resistance of MOSFET (41 m $\Omega$ ),  $I_{d,rms}$  is the effective value of the current passing through MOSFET (2.24A), and D is the duty cycle of 0.5.

#### 3.5.2. Diode loss calculation

The average current passing through the diode  $I_{d,avg} = I_o = 10$  A, and the effective current is  $I_{d,rms} = 7.85$ A. If the forward conduction voltage drop  $V_F$  of the selected diode is 1.0V, the conduction loss is  $P_{cond,diode} = I_{d,rms} V_F [1 - (d/2)] = 5.8$  W. Peak value of diode reverse recovery current  $I_{Rmax} = 10$   $\mu$ A. The reverse bias voltage  $V_{Rmax} = 140$  V, and the time from zero to peak reverse current is approximately equal to the time from peak reverse current to positive recovery current, which is  $t_{rr1} = t_{rr2} = 35$  ns. The shutdown loss is  $P_{sw,diode} = 0.5 V_F I_{Rmax} t_{rr1} f_s + 0.25 V_{Rmax} I_{Rmax} t_{rr2} f_s = 1.24 \times 10^{-6}$  W. Therefore, the total loss of the diode is  $P_{diode} = P_{cond,diode} + P_{sw,diode} \approx 5.8$  W.

#### 3.5.3. Transformer loss calculation

The effective values of the primary and secondary currents are  $I_{p\_RMS} = 2.24$ A,  $I_{s\_RMS} = 7.85$ A. The copper loss of a transformer  $P_{cu,trans} = R_{cu1} I_{p\_RMS}^2 + R_{cs2} I_{s\_RMS}^2 = [2\sigma j N_1 I_{p\_RMS} \sqrt{(\pi A_{e1})}] + [2\sigma j N_2 I_{s\_RMS} \sqrt{(\pi A_{e2})}] = 12.4$  W. The magnetic core loss of the transformer  $P_{core,trans} = \eta f_{eq}^{\beta} B_{peak}^{\beta} V_e = 1.1$  W. Therefore, the total loss of the transformer  $P_{trans} = P_{cu,trans} + P_{core,trans} \approx 12.4$  W + 1.1 W = 13.5 W.

#### 3.5.4. System efficiency calculation

The total loss of the converter is  $P_{loss} = P_{MOSFET} + P_{diode} + P_{trans} = 19.4$  W, while the efficiency  $\eta = P_o / (P_o + P_{loss}) \times 100\% = 96.12\%$ . It can be seen that the efficiency of the system throughout the entire process has reached the required quantity value, indicating that device selection and data selection are reasonable.

### 4. Experiment validation

Full bridge LLC resonant converter to DC/DC has been built. DC/DC parameters are: (1) The input AC voltage of the input link is 220V ( $\pm 5\%$ V), the input filtering inductance is 8mH, the rated output DC voltage is 300V, and the output filtering capacitance is 1100  $\mu$ F; (2) The intermediate link DC/DC converter outputs a given reference voltage of DC 48V and a filtering capacitor of 890  $\mu$ F; and (3) The output link outputs a power frequency three-phase line voltage of 50V, a power of 460W, a filtering inductance of 0.4mH, a filtering capacitor of 32  $\mu$ F, and a three-phase pure resistive load.

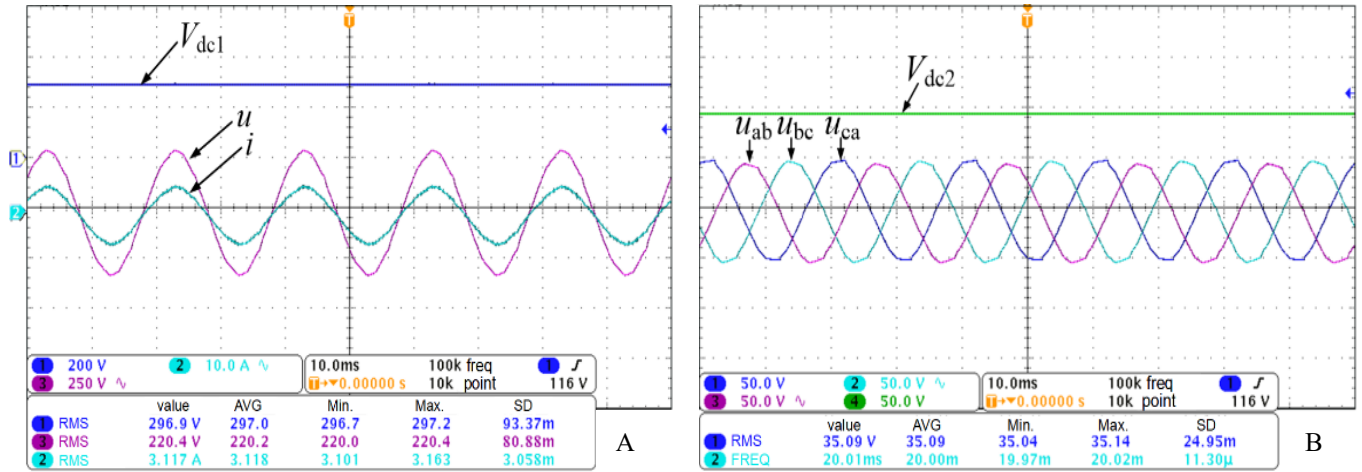


**Figure 2.** The experimental waveform of LLC in  $f_s > f_r$ . (A) The input voltage and current, and the output voltage of the input link. (B) The output voltage of the DC/DC converter and the three-phase voltage of the load.

$u$ ,  $i$ , and  $V_{dc1}$  in **Figure 2A** represent the input voltage and current of the input link, as well as the output DC voltage. For the convenience of comparison, the current waveform here has been expanded by 5 times;  $V_{dc2}$ ,  $u_{ab}$ ,  $u_{bc}$ , and  $u_{ca}$  in **Figure 2B** are the DC voltage and load three-phase voltage output by DC/DC converter respectively. From the simulation results, it can be seen that the 220 V AC voltage is input, and after passing through the LLC converter, DC 48 V is output, and finally, a three-phase sinusoidal AC voltage is output through a three-phase inverter circuit. It can be seen that applying a full bridge LLC resonant converter to DC/DC can achieve basic voltage transformation and energy output functions.

**Figure 3** shows the output ripple voltage waveform of the DC/DC converter under full load. As shown in the figure, the output ripple voltage value is less than 200mV, which meets the ripple value range set during design.

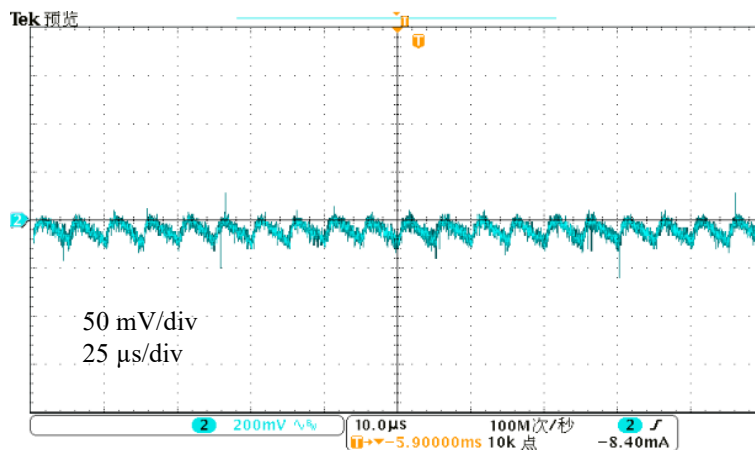


**Figure 3.** Output ripple voltage under full load

**Figure 4** shows the efficiency curves of the experimental device under different conditions. From **Figure 4A**, it can be seen that under full load conditions, the efficiency will also increase with the increase of input voltage. However, when the input voltage exceeds the rated input voltage, the efficiency will decrease. This is because the operating frequency will be greater than the resonant frequency,  $f_s > f_r$  when the input voltage exceeds the rated input voltage, which will affect the ZCS realization of the rectifier diode.

From **Figure 4B**, it can be seen that under the rated input voltage, the efficiency continues to improve as the output current increases. When the rated output current is reached, the efficiency is highest. Efficiency exceeds 93% in all conditions. It can be seen that the designed DC/DC converter meets the design requirements.

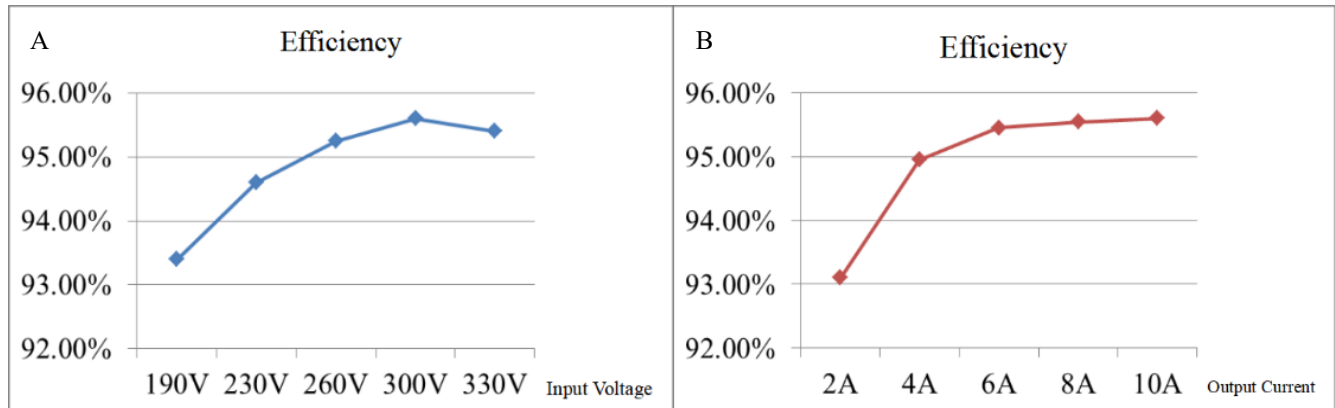


**Figure 4.** Converter efficiency curve. (A) An output current of 10 A load with different input voltages. (B) An input voltage of 300 V with different output currents.

## 5. Conclusion

This article studies the working principle of the LLC resonant full bridge converter, analyzes its operation under optimal conditions, determines the main parameters of the converter, and applies soft switching technology to the DC/DC converter to improve efficiency. The correctness and effectiveness of the theoretical research and design methods of DC/DC converters were verified through prototype experiments.

## Disclosure statement

The authors declare no conflict of interest

## References

- [1] Yoshida D, Kifune H, Hanaka Y, (eds) 2001, IEEE Conference Proceedings Power Electronics and Device Systems, October 25, 2001: ZCS High Frequency Inverter for Induction Heating with Quasi-Constant Frequency Power Control. IEEE, 755–759.
- [2] Sabahi M, Hosseini SH, Sharifian MB, et al., 2010, Zero-voltage Switching Bi-Directional Power Electronic Transformer. IET Power Electr, 5(3): 818–828. <http://doi.org/10.1049/iet-pel.2008.0070>
- [3] Roasto I, Romero-Cadaval E, Martins J, (eds) 2012, Proceedings of IECON 2012-38th Annual Conference on Industrial Electronics Society, October 25–28, 2012: State of the Art of Active Power Electronic Transformers for Smart Grids. IEEE, 5241–5246.
- [4] Posada CJ, Ramirez JM, 2014, Multi-Fed Power Electronic Transformer for Use in Modern Distribution systems. IEEE T Smart Grid, 5(3): 1532–1541. <http://doi.org/10.1109/TSG.2013.2293479>
- [5] Zhao TF, Wang GY, Bhattacharya S, et al., 2013, Voltage and Power Balance Control for a Cascaded H-Bridge Converter-Based Solid-State Transformer. IEEE T Power Electr, 28(4): 1523–1532. <http://doi.org/10.1109/TPEL.2012.2216549>
- [6] Sun G, Gou RF, Sun W, 2016, Research on the Topological Structure and Control Strategy of Power Electronic Transformers Based on MMC Structure. High Volt Electr Appliances, 52(1): 142–147.



- [7] Wang Ting, 2015, Research on Power Electronic Transformers Based on Modular Multilevel Matrix Converters, thesis, Shandong University.
- [8] Mollov SV, Theodoris M, Forsyth AJ, 2004, High Frequency Voltage-Fed Inverter with Phase-Shift Control for Induction Heating. IEE P Electric Power Appl, 151(1): 12–18. <http://doi.org/10.1049/ip-epa:20031058>

**Publisher's note**

Bio-Byword Scientific Publishing remains neutral with regard to jurisdictional claims in published maps and institutional affiliations.